Adsorption of CO_2 on MIL-53(Al): FTIR evidence of formation of dimeric CO_2 species

M. Mihaylov, K. Chakarova, S. Andonova, N. Drenchev, E. Ivanova, E. A. Pidko, A. Sabetghadam, B. Seoane, J. Gascon, F. Kapteijn and K. Hadjiivanov

SUPPORTING INFORMATION

1. Experimental details

The MIL-53(Al) sample used in this study was a commercial BASF product Basolite® A100. To obtain the IR spectra the sample was spread onto a KBr pellet. This technique ensured optimal intensity of the IR bands. Control experiments were performed with a self supporting pellet in order to verify the lack of interaction with KBr. Before the adsorption experiments, the sample was activated by evacuation at 623 K. This temperature was high enough to remove the residual terephthalic acid, as evidenced by the lack of the diagnostic IR band at 1699 cm^{-1} (see Fig. S1, panel B). The IR measurements were performed with Nicolet Avatar 360 and Nicolet 6700 FTIR spectrometers accumulating 64 scans at a spectral resolution of 1 or 2 cm^{-1}. A purpose made IR cell, allowing registering of the spectra between 100 K and ambient temperatures, was used. The cell was connected to vacuum-adsorption apparatus with a residual pressure lower than 10^{-3} Pa. During low temperature experiments, He was introduced in the cell before CO_2 adsorption in order to keep a constant temperature.

Carbon dioxide (99.998 % purity) was supplied by Messer. Labeled $^{13}CO_2$ (^{13}C isotopic purity of 99 atom %) was provided by Aldrich. Helium was supplied by Messer and had a purity of 99.999 %.

2. Computational details

Periodic DFT calculations were performed using the Vienna Ab initio Simulation Package (VASP 5.3.5).[1,2] The exchange-correlation energy was described by the generalized gradient approximation Perdew-Burke-Ernzerhofer (PBE) functional.[3] A plane-wave basis set with a cutoff energy of 500 eV in combination with the projected augmented wave (PAW) method[4] was used. Brillouin zone-sampling was restricted to the Γ point. To account for the van der Waals interactions, the zero damping DFT-D3 dispersion correction method of Grimme was employed.[5] The unit cell parameters for MIL-53(Al) narrow pore (NP) and large pore (LP) forms were previously optimized by us using a multistep cell relaxation procedure for the high-coverage models.[6] The monomeric adsorption complex was modelled using a single MIL(Al)-53-LP (155 atoms), whereas a supercell approach was employed to model the dimer complex. In this case, the periodic model was created by doubling the MIL(Al)-53-NP unit cell along the *a* crystallographic axes. Electronic relaxations were carried out with the tolerances of 10^{-7} eV. The convergence was assumed to be reached when the forces on each atom were below 0.02 eV/Å. A modest Gaussian smearing was applied to band occupations around the Fermi level, and the total energies were extrapolated to $\sigma \rightarrow 0$. Vibrational frequencies were calculated using density functional perturbation theory as implemented in VASP 5.3.5. A scaling factor of 0.9895 was employed. The Hessian matrices for the adsorbed CO_2 molecules only were calculated. The IR intensities were estimated using the script developed by Dr. David Karhánek (http://homepage.univie.ac.at/david.karhanek/downloads.html#Entry02) based on the discussion summarized by Dr. Ralf Tonner.

3. Background spectrum of MIL-53(Al)

The spectra of MIL-53(Al) are already reported in the literature.[7,8] They are characterized by structural μ_2-OH species absorbing at 3708-02 cm^{-1}. These bridging hydroxyls are located at the trans-corner sharing octahedra $AlO_4(OH)_2$ chains. The spectrum of our sample (Figure S1A, spectrum a) is consistent with the previous reports. A sharp band at 3708 cm^{-1} dominates in the OH region. A low-intensity and broad shoulder at ca. 3689 cm^{-1} is also discernible. This shoulder characterizes some OH groups involved in weak H-bonding[9] with residual terephthalic acid or to occluded molecularly adsorbed water.[10]

The spectrum in the 1850 – 400 cm^{-1} region is presented in Fig. S1B. In particular, the strong bands at 1597 and 1445-1417 cm^{-1} are attributed to the antisymmetric and symmetric stretching modes, respectively, of carboxylate groups.[8] The sharp band at 1512 cm^{-1} arises from the C–C ring vibrations. The band at 987 cm^{-1} is due to the deformation modes of bridging hydroxyl groups. Two weak bands at 1024 and 1019 cm^{-1} are assigned to the δ(CH) (ν_{18a}) modes of the terephthalate ligands.[8] The position of this band is indicative of the large pore (1024 cm^{-1}) and narrow pore (1019 cm^{-1}) forms of the MOF structure. The results indicated the co-presence of the two forms in our sample.

Because part of the adsorption experiments were performed at low temperature, it is important to know the temperature/pressure effect on the background spectra. Temperature hardly affects the spectra in the low-frequency region but has a strong effect on the spectra in the OH stretching region. At 100 K and in presence of He the OH band shifts to higher frequencies and splits into two components at 3720 and 3712 cm^{-1} (Figure S1A, spectrum b). The higher frequency component is associated with the large pore, and the lower frequency, with the narrow pore structure of this MOF.[11]

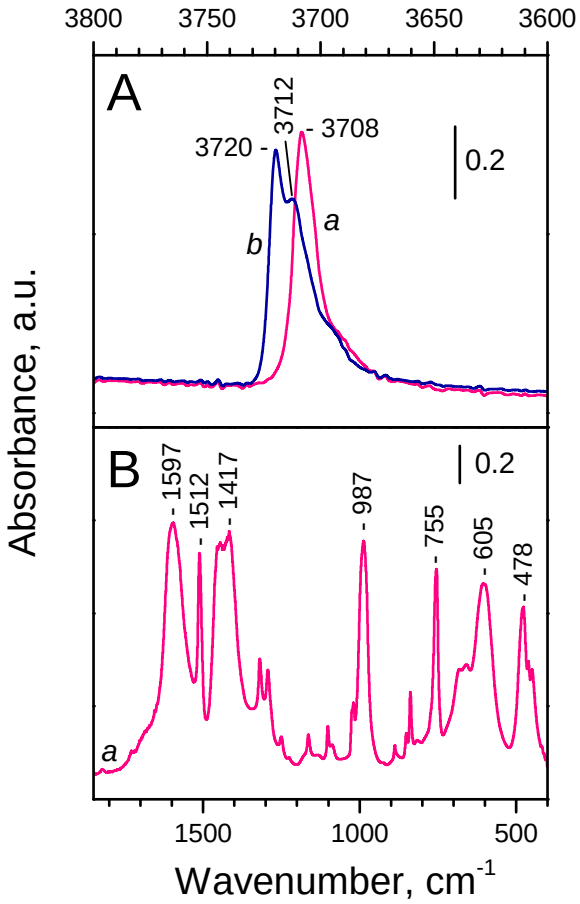

Figure S1. FTIR spectra of the activated MIL-53(Al) sample at ambient (a) and low temperature (b). Panel A: hydroxyl stretching region; Panel B: 1850 - 400 cm^{-1} region.

Adsorption of CO_2

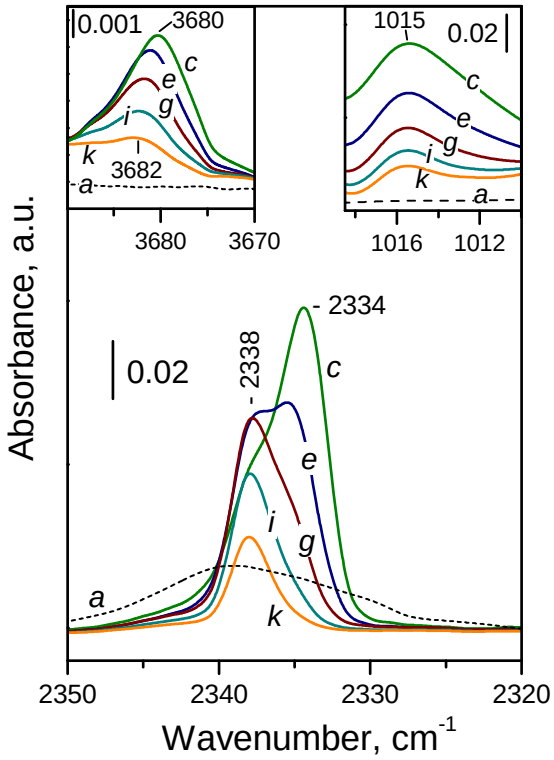

Figure S2. FTIR spectra registered after adsorption of $^{12}CO_2$ at 100 K on MIL-53(Al). The notation of the spectra is the same as in Fig. 1 from the main text. The left inset shows changes in the ν(OH) region, and the right inset, in the δ(OH) region. The spectra are background and gas-phase corrected.

Changes in the ν(OH) region induced by CO_2 adsorption are shown on the left inset in Fig. S2. The original OH bands are not shown because their maxima move with the temperature change during the evacuation process. The right panel shows changes in the δ(OH) region.

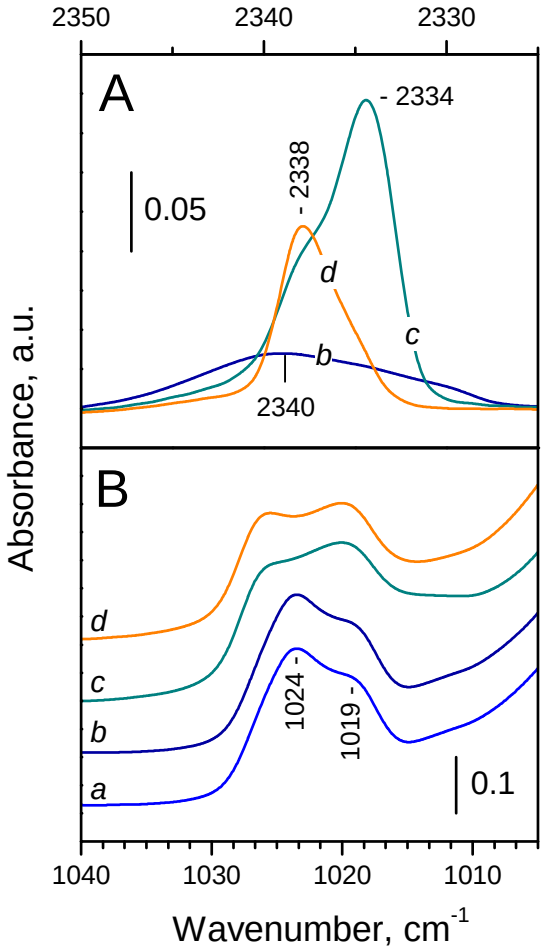

Figure S3. FTIR spectra registered after adsorption of $^{12}CO_2$ at 100 K on MIL-53(Al). Panel A shows background-corrected spectra in the $\nu_{as}(CO_2)$ region, while panel B, original spectra in the 1040-1005 cm^{-1} region. Spectra "b", "c" and "d" correspond to spectra "d", "c" and "h" from Fig. 1, while spectrum "a" is registered before CO_2 adsorption.

Figure S3B shows the original spectra in the 1040-1005 cm^{-1} region, where the δ(CH) modes of the terephthalate ligands are observed. The position of this band is indicative of the large pore (1024 cm^{-1}) and narrow pore (1019 cm^{-1}) forms of the MOF structure.[8] It is seen that before CO_2 adsorption the large pore form is predominant and formation of CO_2 dimmers (Fig. S3, spectrum c) provokes a partial conversion of the material into the narrow pore form.

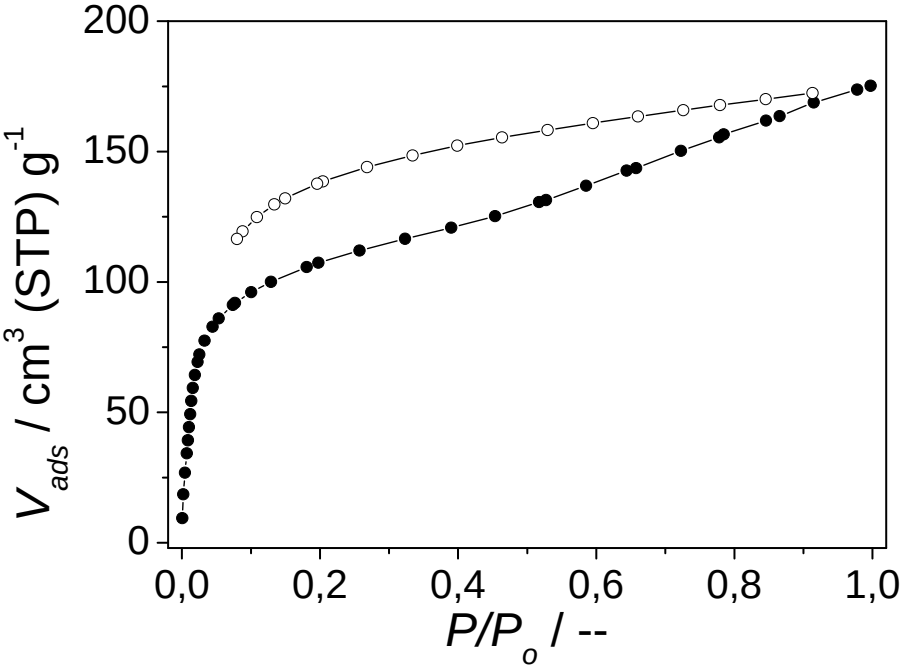

Figure S4. CO_2 adsorption-desorption isotherms on MIL-53(Al) at 195 K. Closed symbols represent the adsorption, and open symbols, the desorption branches.

Fig. S4 presents the CO_2 adsorption-desorption isotherms on MIL-53(Al) at 195 K. The adsorption proceeds in steps and desorption occurs with hysteresis, the adsorption-desorption isotherms displaying a hysteresis loop. The results indicate breathing behaviour of the material at this temperature.[12]

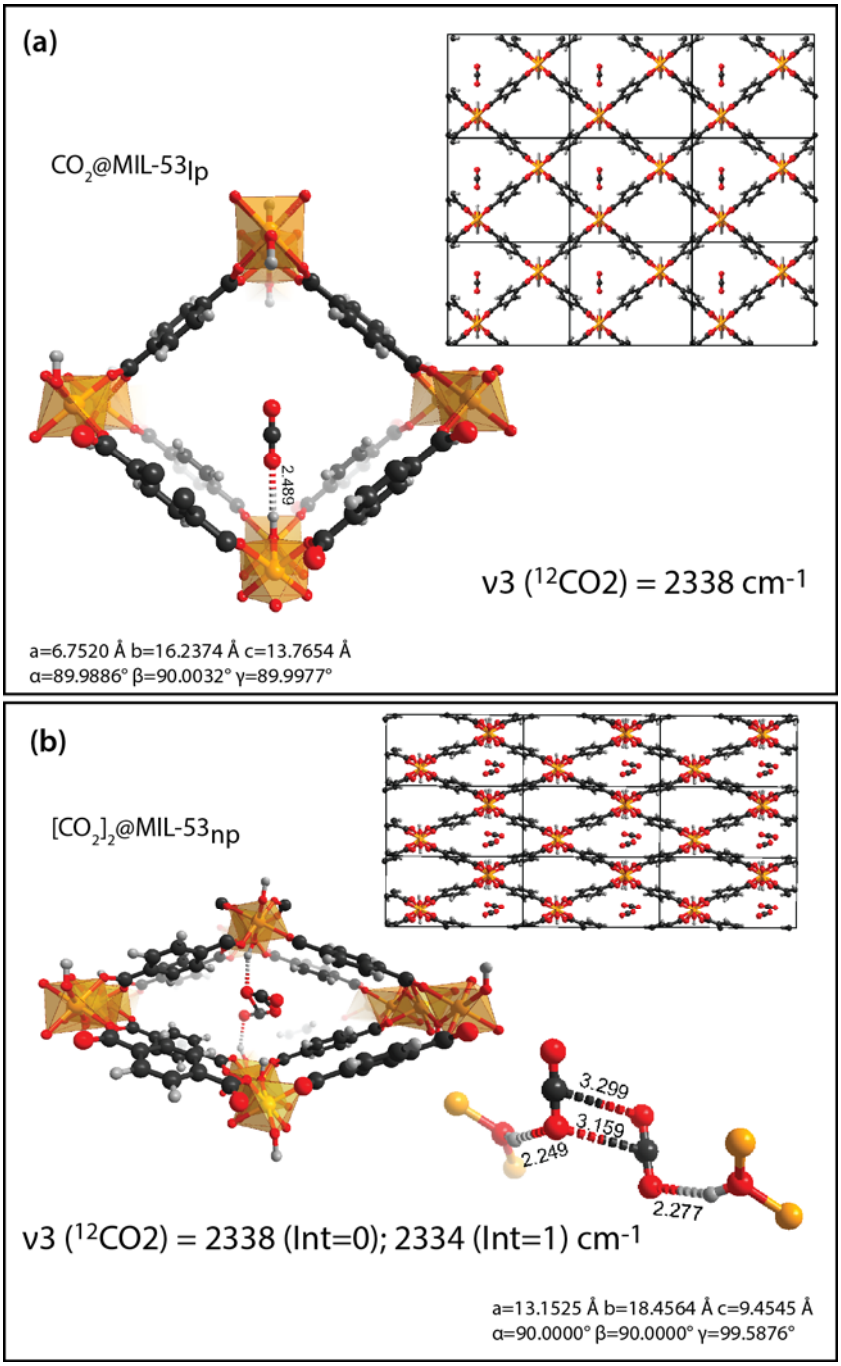

Figure S5. Optimised structure of CO_2 monomer (a) and dimer (b) adsorption complexes in the large-pore and narrow-pore structures of MIL-53(Al), respectively. Selected interatomic distances are given in angstrom. The colour scheme is the same as in Fig. 4.

References

1. G. Kresse and J. Hafner, *Phys. Rev. B.* 1993, **48**, 13115; *Phys. Rev. B.* 1994, **49**, 14251.
2. G. Kresse and J. Furthmüller, *Comput. Mater. Sci.* 1996, **6**, 15; *Phys. Rev. B.* 1996, **54**, 11169.
3. J.P. Perdew, K. Burke and M. Ernzerhof, *Phys. Rev. Lett.* 1996, **77**, 3865.
4. P. E. Blöchl, *Phys. Rev. B*, 1994, **50**, 17953.
5. S. Grimme, J. Antony, S. Ehrlich, and S. Krieg, *J. Chem. Phys.* 2010, **132**, 154104.
6. E. Stavitski, E. A. Pidko, S. Couck, T. Remy, E. J. M. Hensen, B. M. Weckhuysen, J. Gascon and F. Kapteijn, *Langmuir* 2011, **27**, 3970.
7. U. Ravon, G. Chaplais, C. Chizallet, B. Seyyedi, F. Bonino, S. Bordiga, N. Bats and D. Farrusseng, *ChemCatChem* 2010, **2**, 1235.
8. C. Volkringer, T. Loiseau, N. Guillou, G. Ferey, E. Elkaim, A. Vimont, *Dalton Trans.* 2009, 2241.
9. K. Hadjiivanov, *Adv. Catal*., 2014, **57**, 99.
10. C. Volkringer, H. Leclerc, J.-C. Lavalley, T. Loiseau, G. Férey, M. Daturi, A. Vimont, *J. Phys. Chem. C* 2012, **116**, 5710.
11. M. Mihaylov, S. Andonova, K. Chakarova, A. Vimont, E. Ivanova, N. Drenchev and K. Hadjiivanov, *Phys. Chem. Chem. Phys.* 2015, **17**, 24304.
12. M. Alhamami, H. Doan and C.-H. Cheng, *Materials* 2014, **7**, 3198.